Geological Society of America Bulletin

Experimental Study of Unconfined Flow of Solnhofen Limestone at 500° to 600°C

ERNEST H. RUTTER and STEFAN M. SCHMID

Geological Society of America Bulletin 1975;86;145-152
doi: 10.1130/0016-7606(1975)86<145:ESOUFO>2.0.CO;2

Experimental Study of Unconfined Flow of Solnhofen Limestone at 500° to 600°C

ERNEST H. RUTTER *Geology Department, Imperial College, London SW 7, England*
STEFAN M. SCHMID *Australian National University, Research School of Earth Sciences, P.O. Box 4, Canberra, Australia*

ABSTRACT

Results of 25 uniaxial creep, stress-relaxation, and constant strain-rate tests in the temperature range 500°C to 600°C on cylinders of Solnhofen limestone are reported. Permanent strains of as much as 20 percent were often produced. Standard experimental procedures for metallurgical creep tests were used. The results of different experimental techniques employed on unconfined rock were found to be consistent and were comparable with data from high-temperature triaxial tests on the same rock. The strength of this rock, extrapolated to geological strain rates, was found to be high compared with stress levels expected in nature. *Key words: structural geology, rock mechanics, carbonate rocks, deformation, overthrusts.*

INTRODUCTION

This paper reports the results of 25 uniaxial compression creep, relaxation, and constant strain-rate tests at high temperature on Solnhofen limestone, a fairly homogeneous, fine-grained (10 to 20μm) calcite rock. Experiments were performed in the temperature range 500°C to 600°C (from about 0.48 to 0.54 of the absolute melting temperature of calcite). At about 0.5 T_m (half of the absolute melting temperature) calcite rocks become ductile, even at atmospheric pressure (Heard, 1960; Rutter, 1972c), and permanent strains of at least a few percent may be induced before fracture or disaggregation. Ductility of calcite rocks at low pressures and high temperatures involves a mixture of intracrystalline and cataclastic (grain fracturing, rotation, and sliding) flow processes. Heard and Raleigh (1972) suggested that self-diffusion is the deformation-rate limiting process for steady-state intracrystalline flow in the temperature range of interest here. In planning these uniaxial experiments, we hoped to detect a change in the balance between cataclastic and intracrystalline processes over a range of strain rates, so that high-temperature intracrystalline flow could be studied using a simpler apparatus than a high-temperature triaxial rig. This objective proved to be partly successful.

The experiments were designed to apply to a rock some of the empirical methods employed by Dorn and his co-workers (1957; review by Garofalo, 1965) for various metals. An outline of the theoretical basis of the experiments is given below.

Results of the uniaxial tests on Solnhofen limestone are compared with results of a series of triaxial tests on the same rock, carried out both dry and in the presence of interstitial water (Rutter, 1974).

Pore compaction and (or) the sequence of dehydration reactions of progressive regional metamorphism can, and probably generally do, elevate pore fluid pressure in rocks until it equals or exceeds the least principal stress (Hubbert and Rubey, 1959; Raleigh and Paterson, 1965; Heard and Rubey, 1966; Price, 1970; Price and Hancock, 1972; Rutter, 1972c). Such conditions may favor frictional sliding and cataclastic behavior even at elevated temperatures. Thus a zero effective confining pressure, corresponding to an unconfined laboratory test, is not necessarily a geologically unrealistic condition, as is commonly believed. It is shown that the data collected from high-temperature uniaxial experiments on Solnhofen limestone may be used (with certain reservations) as a basis for extrapolation to geological conditions, and the resulting geological implications are discussed.

THEORETICAL BASIS OF EXPERIMENTS

Dorn (1957) has shown that the constitutive flow law for thermally activated plastic flow of metals can be written as

$$\dot{e} = A \exp(-H/RT) f_1(\sigma) f_2(S) \qquad (1)$$

where $\dot{e}$ is the strain rate at differential stress σ and temperature T. R is the gas constant, H is the activation enthalpy for creep, and A is a constant that incorporates the frequency of attempts at the activation barrier, the strain per successful activation, the entropy of activation, and the shear modulus. S is a description of those structural features of the material that affect strain rate, for example, the arrangement and nature of point and line defects and grain boundaries.

Dorn proposed various experimental techniques whereby the parameters and functions of this equation might be determined, and he emphasized the need for structure to be held constant when determining the relation between strain rate and stress. By taking logarithms of equation (1) and differentiating with respect to $1/T$ at constant structure and stress, we obtain

$$H = -R \left(\frac{\delta \ln \dot{e}}{\delta\, 1/T} \right)_{S,\sigma}, \qquad (2)$$

which, for a small temperature interval, $T_2 - T_1$, can be approximated by

$$H = -R \frac{\ln (\dot{e}_{T_1}/\dot{e}_{T_2})}{1/T_1 - 1/T_2}. \qquad (3)$$

This expression leads to a method for the determination of H. If the test temperature can be instantaneously changed after a certain amount of creep strain at constant stress, there will be an instantaneous change in strain rate. Immediately before and after the temperature change, the structure can be assumed to be constant. Transient creep is defined as a continuous decrease in creep rate at constant stress. The very fact that transient creep occurs in materials means that structural changes occur during creep. Creep at constant strain rate under constant stress (steady-state creep), or over small strain increments during transient creep, occurs at constant structure. Using the differential temperature creep test, activation enthalpy for flow can be investigated even in the transient creep region as a function of strain and hence of structure. Most of the experiments described in this paper are differential temperature creep tests. It should be noted that in deriving equation (3) it is assumed that the shear modulus is temperature independent between T_1 and T_2, so that A is truly constant.

Geological Society of America Bulletin, v. 86, p. 145–152, 9 figs., February 1975, Doc. no. 50201.

In these experiments, the relation between strain rate and stress has been investigated in two ways: (a) by plotting log stress or stress against log strain rate at an arbitrary level of strain in the steady-state creep region and (b) from stress-relaxation experiments. It has long been known that the strain-rate sensitivity of stress for metals (review by Garofalo, 1965) deformed at and above 0.5 T_m can be described by

$$\dot{e} = B \exp (C\,\sigma) \tag{4}$$

or

$$\dot{e} = B' \sinh (C'\,\sigma) \tag{5}$$

at relatively high stress levels (above about $\sigma = 10^{-3}\ \mu$; Weertman, 1968), where μ is the shear modulus, and

$$\dot{e} = D\,\sigma^n \tag{6}$$

at relatively low stress levels. Data described by equations (4) and (5) are linear on a plot of stress against log strain rate, and equation (6) is linear in the log stress against log strain-rate coordinate frame. In these equations, B, C, B', C', D, and n are empirical constants. A stress-strain rate relation of the form of equation (6) was obtained theoretically by Weertman (1968) for steady-state creep, where n ranged from 3 to 6, and the activation enthalpy for creep was equal to that for self diffusion. Heard and Raleigh (1972) have demonstrated creep by dislocation climb controlled polygonization in Yule marble at temperatures of 500°C and above at differential stress levels below 800 bars, with the exponent n approximately equal to 8.

The stress-strain rate relation for Solnhofen limestone was investigated from five stress-relaxation experiments, where stress was observed as a function of time while the specimen was held (ideally) at constant strain. In this type of experiment, a small amount of elastic strain is converted into permanent strain. Raleigh and Kirby (1970) and Raleigh and others (1971) used this type of test with samples of olivine in solid pressure-medium apparatus. If the apparatus plus specimen displacement is held constant, as the specimen relaxes the compressed apparatus will extend and, therefore, the specimen will shorten; that is, a portion of the elastic energy of the specimen plus apparatus is converted into permanent strain in the specimen. Thus the permanent strain rate in the specimen, $\dot{e}_s$, assuming strains to be small so that they can be regarded as additive, is given by

$$\dot{e}_s = (L_a K_a + K_s)\,\frac{d\sigma}{dt} \tag{7}$$

where K_a and K_s are the elastic compliances of the apparatus material and the specimen, respectively, and L_a is a constant to convert apparatus displacements into equivalent specimen strain. For the power law relation between stress and strain rate,

$$\log \dot{e}_s = \log D + n \log \sigma \tag{8}$$

therefore

$$\log (L_a K_a + K_s) + \log \frac{d\sigma}{dt} = \log D + n \log \sigma\,. \tag{9}$$

Differentiating with respect to $\log \sigma$ gives

$$\frac{d\left(\log \frac{d\sigma}{dt}\right)}{d\,(\log \sigma)} = n\,, \tag{10}$$

which can be used to determine n from the data of a stress-relaxation test. Similarly, for the exponential stress–strain-rate relation,

$$\frac{d\left(\log \frac{d\sigma}{dt}\right)}{d\sigma} = C/\ln(10)\,. \tag{11}$$

In each case the stiffness of the apparatus can be neglected, provided that it remains constant.

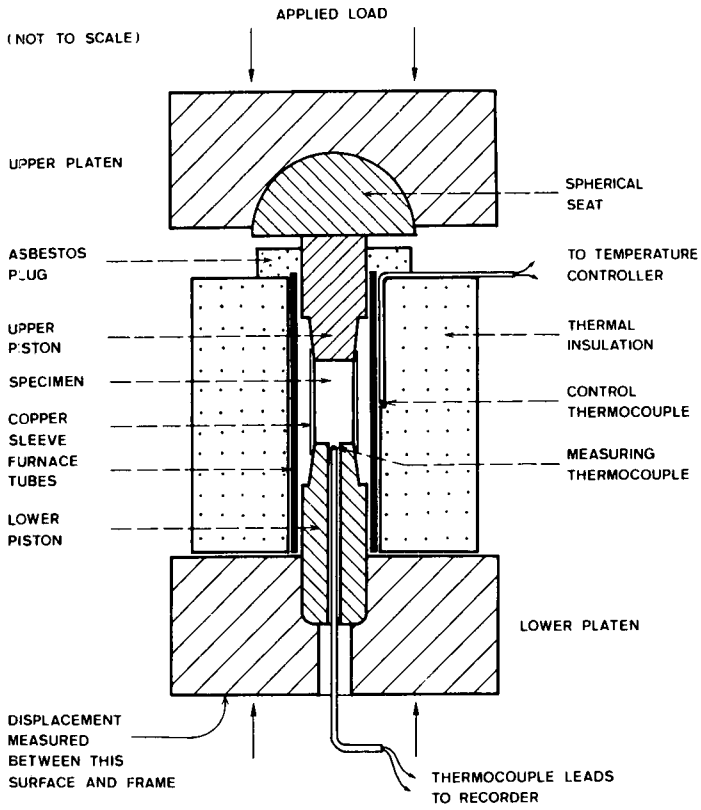

Figure 1. Diagram of the furnace-specimen assembly.

Methods used by metallurgists for the determination of strain-rate sensitivity to stress involve experimental precautions to ensure that the determination is made at constant structure (Dorn, 1957). Such precautions have not been taken in studies on rocks. It has generally been assumed that structure is virtually constant over limited ranges of temperature and stress, and depends mainly on

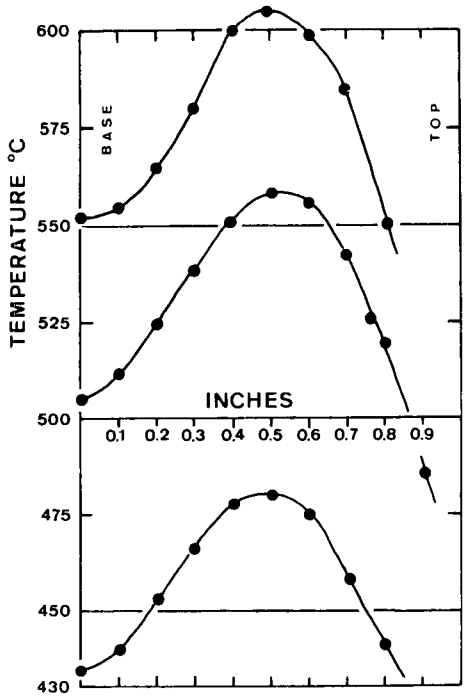

Figure 2. Axial thermal gradients along a hollow sample of Solnhofen limestone at various temperatures.

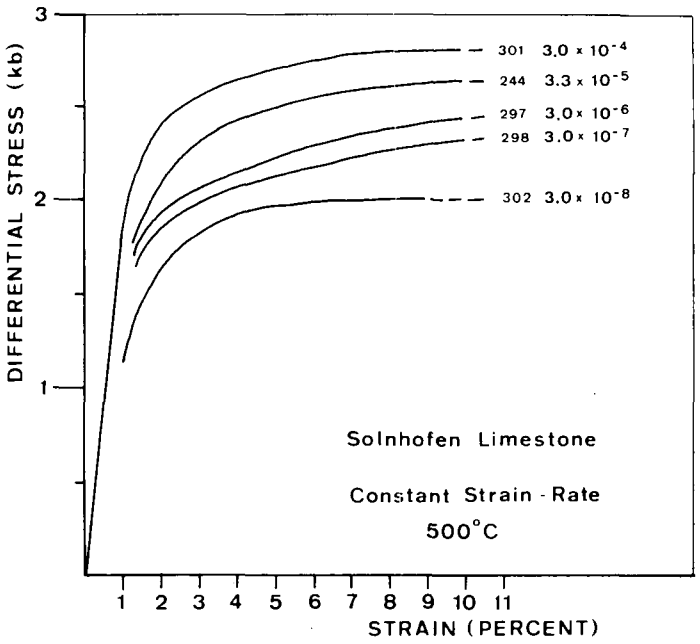

Figure 3. Stress against strain curves from constant strain-rate tests at 500°C.

strain. Determination of strain-rate sensitivity to stress from creep tests on different specimens at different applied stresses involves this assumption. If the assumption is invalid, then the experimentally determined strain-rate sensitivity to stress incorporates the stress-dependent structure factor. Recovery during deformation invalidates the constant structure assumption.

Short-term stress-relaxation experiments, in which the induced plastic strain is small, give a constant structure strain-rate sensitivity to stress, provided there is no recovery. Li (1967) has shown that, if dislocation velocity is related to thermal (effective) stress, σ^*, by a power law with stress exponent m^*, stress-relaxation data are described by

$$\sigma^* = \sigma - \sigma_\mu = E\,(t + c)^{-1/(m^* - 1)}, \qquad (12)$$

where σ is the applied stress at time t, σ_μ is the long-range internal (athermal) stress, and E and c are constants. A plot of log σ against log $(t + c)$ is linear over short times (less than 10^3 sec) and its slope, s, is related to n by $n = (s - 1)/s$. At long times, σ becomes asymptotic to σ_μ.

If recovery occurs during stress relaxation, σ decreases continually with time because σ_μ decreases during the recovery. A value of n determined from such data incorporates the stress-dependent structure factor. Strictly, a figure for the strain-rate sensitivity to stress obtained under conditions of varying structure is valid only within the range of experimental conditions. There is no firm theoretical basis for extrapolation beyond them. Though it is interesting to discuss the possible geological implications of such extrapolations, they should be treated with caution.

APPARATUS

Creep experiments were performed using a five-ton capacity, commercial creep-testing machine, in which loads were applied through a system of levers. Specimens were heated by a small electric resistance furnace. A schematic diagram of the furnace-specimen assembly is shown in Figure 1.

Using an electric motor driven system, initial loading was achieved over a period of ~1 hr at a constant displacement rate. Slow loading was used, because it was found that rapid loading often resulted in premature failure of the sample.

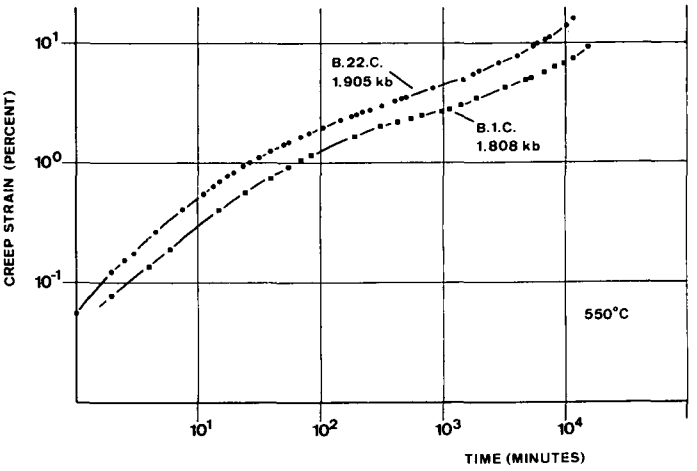

Figure 4. Log strain against log time plot for complete creep tests B.1.C. and B.22.C. Both tests were performed at constant temperature, but B.1.C. was rapidly loaded and B.22.C. was slowly loaded at constant displacement rate.

To employ the differential temperature technique successfully in these experiments, it was necessary to be able to change the temperature rapidly, which in turn meant using a furnace-specimen assembly of low thermal capacity and small physical size. Unfortunately, large thermal gradients along the sample had to be tolerated. The thermal gradient along a sample is shown in Figure 2 for test temperatures similar to those used. The specimen temperature was only reasonably constant over about half of the sample, falling off rapidly at the ends but very rapidly at the top. However, it is evident that when the temperature was changed, each point along the sample changed by the same amount. Examination of deformed specimens revealed that significant deformation occurred only in the lowermost 1.8 cm (0.7 in.) of the initially 2.54-cm (1.0-in.) long sample. Specimen temperatures quoted are arithmetic averages of those measured at points along the sample, and these figures correspond with the true figure at points on the sample about 1.26 cm (0.5 in.) apart. Strains and strain rates, calculated assuming the effective original specimen length to have been one-half of the true specimen length, were considered to have been representative of the average deformation of the sample. The same result was obtained by summing strain rates estimated for isothermal pill-shaped elements along the specimen length. The arrangement employed, though producing a poor thermal gradient, permitted temperature changes of 50°C to be achieved in about 5 min.

Creep displacements were measured using a direct reading dial gauge together with a linear variable differential transformer with a resolution of 2.5 × 10^{-6}cm (10^{-6} in.). Because large creep strains (more than 10 percent) were induced in most samples to maintain approximately constant stress conditions (Rutter, 1972b), the load on the sample was increased manually by 0.05 percent following each 0.05 percent increase in creep strain.

The constant strain-rate tests were performed in testing machines described in Heard (1963) and Rutter (1972a, 1972b). The experiments were performed without any confining pressure but with 0.35-mm (0.01 in.) wall-thickness annealed copper sleeves around the sample, similar to those employed on the creep machine (Fig. 1). In this apparatus, specimen temperature gradients were typically ± 1.5°C over the specimen length. The massive steel test cylinder prohibited differential temperature tests.

Test specimens of 1.26 cm (0.5 in.) diameter by 2.54 cm (1.0 in.) long were used for the creep tests, and specimens 0.95 cm (0.375 in.) diameter by 1.9 cm (0.75 in.) long for the constant strain-rate tests. It had already been established (Rutter, 1972c) using the constant strain-rate apparatus that there were no significant differences in the mechanical behavior of samples of the two sizes.

TABLE 1. RESULTS OF THE CREEP TESTS

Test	Stress (kb)	Temp (°C)	Strain rate (sec^{-1}) 4 %*	6 %*	8 %*	10 %*
B.16.C.	1.585	600	1.8×10^{-7}	4.0×10^{-7}	1.9×10^{-7}	
		550	8.4×10^{-9}	1.4×10^{-8}	6.4×10^{-9}	
B.13.C.	1.623	600	3.5×10^{-6}	7.6×10^{-7}	4.2×10^{-7}	4.6×10^{-7}
		550	5.4×10^{-8}	2.6×10^{-8}	2.0×10^{-8}	1.9×10^{-8}
B.14.C.	1.696	600	1.7×10^{-5}	7.6×10^{-7}	4.7×10^{-7}	
		550	7.8×10^{-8}	3.6×10^{-8}	1.4×10^{-8}	
B.11.C.	1.802	600	5.5×10^{-6}	3.0×10^{-6}	2.4×10^{-6}	2.0×10^{-6}
		550	9.2×10^{-8}	5.4×10^{-8}	4.0×10^{-8}	3.6×10^{-8}
B.1.C.	1.808	550	1.3×10^{-7}	1.7×10^{-7}	1.4×10^{-7}	1.2×10^{-7}
		500			3.7×10^{-9}	
B.9.C.	1.880	600		1.4×10^{-5}	7.2×10^{-6}	4.8×10^{-6}
		550	6.0×10^{-7}	2.5×10^{-7}	1.2×10^{-7}	
		500	9.8×10^{-9}	4.9×10^{-9}	2.4×10^{-9}	
B.12.C.	1.905	600		1.8×10^{-5}	1.1×10^{-5}	7.4×10^{-6}
		550	1.8×10^{-5}	4.9×10^{-7}	3.1×10^{-7}	2.1×10^{-7}
		500	5.0×10^{-8}	1.2×10^{-8}	9.0×10^{-9}	
B.22.C.	1.905	550	2.4×10^{-6}	4.3×10^{-7}	2.4×10^{-7}	1.7×10^{-7}
B.21.C.	1.937	600		2.2×10^{-5}	1.5×10^{-5}	1.2×10^{-5}
		550	1.2×10^{-6}	4.0×10^{-7}	3.1×10^{-7}	3.2×10^{-7}
		500		1.9×10^{-8}	1.5×10^{-8}	1.4×10^{-8}
B.17.C.	1.944	600		1.1×10^{-4}	5.5×10^{-5}	
		550	8.6×10^{-6}	1.7×10^{-6}	8.4×10^{-7}	
B.20.C.	1.950	550	9.2×10^{-7}			
B.18.C.	1.980	600			6.6×10^{-5}	6.1×10^{-5}
		550		2.9×10^{-6}	1.2×10^{-5}	1.1×10^{-6}
		500			2.9×10^{-8}	2.7×10^{-8}
B.23.C.	1.980	600			1.5×10^{-5}	1.3×10^{-5}
		550	7.2×10^{-7}	3.2×10^{-7}	2.7×10^{-7}	2.4×10^{-7}
B.5.C.	2.010	550	4.9×10^{-6}	3.9×10^{-6}	4.0×10^{-6}	3.2×10^{-6}
		500		7.4×10^{-8}	5.7×10^{-8}	4.3×10^{-8}
B.6.C.	2.077	550		8.6×10^{-6}	6.4×10^{-6}	

* *Total strain at which given strain rate was determined.*

TABLE 2. LINEAR REGRESSION ANALYSES—RELAXATION DATA

Test	Slope $kb^{-1} \log_{10} sec^{-1}$	SD* of slope	Intercept (log stress rate)	SD* of mean	Mean log stress rate log bar sec^{-1}	Mean stress (kb)	No. obs.†
Exponential							
B.21.C.	4.257	0.057	-8.930	0.006	-1.840	1.667	29
B.12.C.	3.485	0.067	-7.950	0.007	-2.126	1.671	32
B.23.C.	3.268	0.054	-7.397	0.004	-2.165	1.601	60
B.18.C.	3.636	0.053	-7.667	0.005	-1.692	1.643	38
B.22.C.	3.285	0.135	-7.248	0.011	-2.172	1.545	54
Power							
B.21.C.	16.60	0.199	-5.501	0.066	-1.840	0.221	29
B.12.C.	13.70	0.142	-5.170	0.068	-2.126	0.222	32
B.23.C.	12.30	0.080	-4.670	0.064	-2.165	0.203	60
B.18.C.	13.85	0.093	-4.650	0.067	-1.692	0.213	38
B.22.C.	12.62	0.115	-4.520	0.130	-2.172	0.180	54

* *SD = standard deviation.*
† *Number of observations.*

EXPERIMENTAL RESULTS

The results of all experiments performed are summarized in Tables 1 and 2 and in Figure 3. The data of all the creep tests were plotted manually and values for the tables were extracted from the plots. The applied stresses and the strain rates at particular creep strains at the appropriate temperatures are shown for each creep test in Table 1. By way of graphic example, log strain–log time plots of two complete creep tests are shown in Figure 4. Figure 5 shows a log strain rate against strain plot for a complete creep test and for a differential temperature creep test performed at the same stress level.

Five of the creep tests performed at high stress levels were completed by performing stress-relaxation tests. The data of the two most extreme of these tests are shown in Figure 6.

Constant strain-rate tests were performed over the strain-rate range 3×10^{-4} sec^{-1} to 3×10^{-8} sec^{-1} at 400°C and 500°C. The results of the 500°C tests are shown in Figure 4. At 400°C, the rock exhibited brittle behavior in the constant strain-rate apparatus. The stresses and strain rates were higher than could be achieved in the creep apparatus. It is believed that premature failure (mentioned above) at high loading rates on the creep machine occurred because, due to the higher thermal gradient along the sample, unstable cracks could propagate from the cooler regions. In the constant strain-rate machine at 500°C, Solnhofen limestone could be deformed beyond 10 percent strain without fracture even at the highest strain rate attainable.

DISCUSSION OF EXPERIMENTAL RESULTS

Form of the Creep Curve

From Figure 4 it is seen that portions of the creep curve can be represented by a power law of the form

$$e = \beta t^m , \qquad (13)$$

where e is the creep strain, t is the time, and β and m are parameters. The initial value of m was high, 0.825, and settled down to a minimum of about 0.33. In the region of 5 percent creep strain, m increased again and approached 1.0 (steady-state creep). A similar pattern of behavior was noted in all the experiments.

Each temperature change (during which the load was maintained) was accompanied by a period of transient creep (Fig. 5). This transient creep persisted for about 100 min and exhibited a similar form whether the temperature was increased or decreased, regardless of the strain rate being investigated. It is possible that the sudden temperature change produced recoverable damage to the specimen. The initial high rates of transient creep (with high m values) generally observed immediately after loading may perhaps be interpreted in the same way. Despite the transients, the 550°C portions of a differential temperature creep test eventually settled down to coincide with the complete creep curve obtained at the same temperature and stress level (Fig. 5). Similar effects occur in differential temperature tests on metals and organic polymers (McCrum and Pearce, 1973).

Activation Enthalpy for Creep

Assuming that the transient creep associated with the temperature changes in the differential temperature creep tests may be neglected, activation enthalpies for creep can be computed from equation (3). A total of 54 determinations of activation enthalpy were made from 50°C temperature changes within the 500°C to 600°C temperature range (Fig. 7). It is evident that the activation enthalpy is independent of strain, a fact which Dorn (1957) noted for metals. Dorn pointed out that this meant that the various operative deformation mechanisms contributed to the accumulation of strain in the same ratio at all strains. This constancy of activation enthalpy mitigates against the applicability of exhaustion theories of creep (Garofalo, 1965), which require that activation energy increase with strain.

It may be noted that these data lend support to the technique used for the determination of activation enthalpy from constant strain-rate tests. In this method, stress at an arbitrary level of strain is plotted against log strain rate at various temperatures, and activation enthalpy is calculated from the separation of the resulting isotherms at constant stress (Heard, 1963; Heard and Raleigh, 1972; Carter and Avé Lallemant, 1970; Rutter, 1974).

It is evident that there is a tendency for activation enthalpy to decrease with decreasing strain rate (Fig. 7b) and because of the fact that strain rate depends on temperature and stress, there are also variations of activation enthalpy with the latter parameters. From these data it may be inferred that there is a change in the balance between different deformation mechanisms as strain rate or stress is lowered.

The mean of all the activation enthalpy values is 90.4 ± 8.1 kgcal $mole^{-1}$ (one standard deviation). This figure may be compared with Anderson's (1969) figure of 88.0 kgcal $mole^{-1}$ for self-diffusion in calcite, obtained at atmospheric pressure in the same temperature range by an isotopic exchange method. Both of these figures, however, are high compared with activation enthalpy

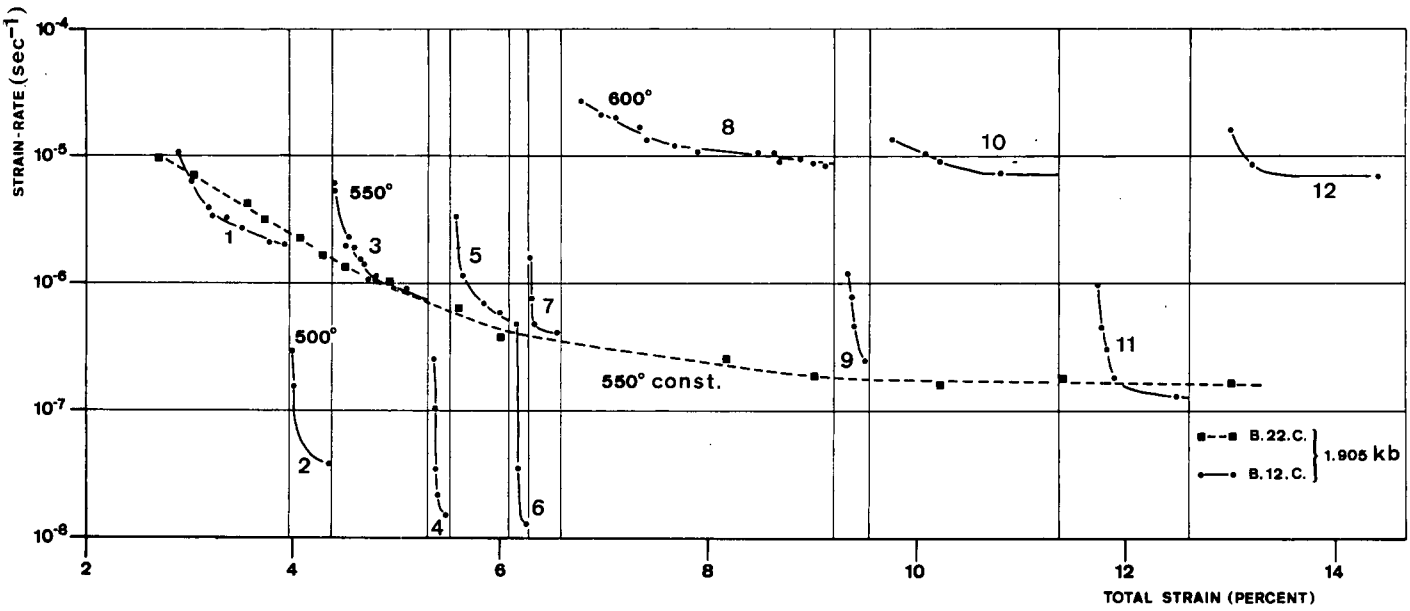

Figure 5. Log strain rate against strain plot of a differential temperature creep test (B.12.C., numbered segments of curves) and a complete creep test (B.22.C.) performed at the same stress level. Vertical lines show strain levels at which temperature was abruptly changed during test B.12.C. Creep curves shown are based on many more measurements than are actually plotted in figure, especially at low strain-rate end of each constant temperature segment.

figures for the creep of calcite rocks under 3 to 4 kb mean pressure (including Solnhofen limestone from the same block): 60.7 ± 1.3 kgcal mole^{-1}: Yule marble T cyl, Heard and Raleigh, 1972; 62.0 ± 1.3 kgcal mole^{-1}: Yule marble 1 cyl, Heard and Raleigh, 1972; 62.1 ± 5.8 kgcal mole^{-1}: Carrara marble, Rutter, 1974; 47.1 ± 4.5 kgcal mole^{-1}: Solnhofen limestone, Rutter, 1974; (confidence limits at one standard deviation).

Anderson (1972) showed that the relative diffusivities of carbon and oxygen in calcite are different under different hydrostatic pressures, but there are no comparative activation enthalpy data. It must be borne in mind that a variation in the nature of diffusing species for diffusion controlled flow in calcite at different mean pressures may lead to different activation enthalpies for flow.

It can alternatively be argued that the tendency for activation enthalpy for flow to decrease with decreasing strain rate allows the possibility that it might level off at 50 to 60 kgcal mole^{-1} at a low strain rate. The observed higher activation energy may only be due to a component of cataclastic deformation, which would be suppressed by deformation at a lower strain rate or at a higher confining pressure.

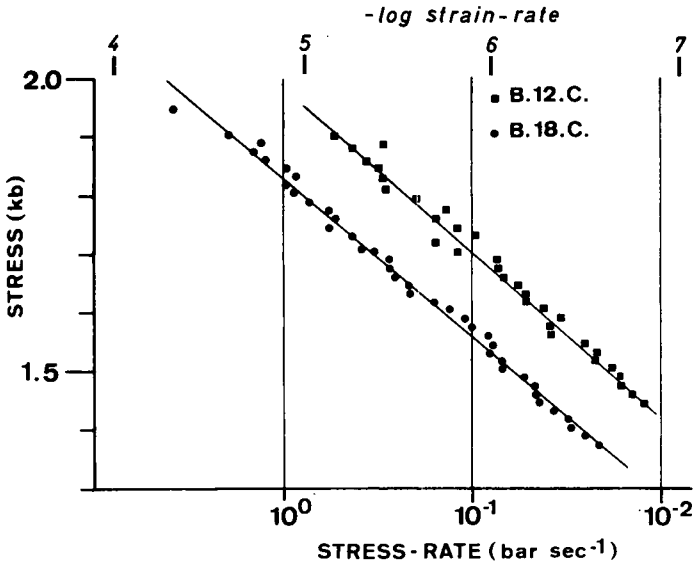

Figure 6. Stress relaxation curves obtained at 600°C. Only the two most extreme curves are shown. Strain-rate scale associated with stress rates at top of diagram.

Stress Dependence of Strain Rate

Figure 8 shows a plot of differential stress against −log strain rate at 8 percent total strain for Solnhofen limestone. In addition to the creep and constant strain-rate data obtained under uniaxial conditions, we plot data obtained under triaxial conditions (Rutter, 1974) on the same rock with a confining pressure of 1.5 kb. It may be seen that the 500°C uniaxial constant strain-rate data are consistent with the creep data, and that the 500°C triaxial data, when extrapolated, would probably coincide with the uniaxial data at a strain rate of about 10^{-8} sec^{-1}; that is, at this strain rate and below, the strength of the rock would be independent of confining pressure.

The stress-relaxation data obtained at 600°C probably give the more reliable indication of the rate of change of strain rate with stress because (1) there is less scatter due to specimen variability and (2) the data extend into regions of lower stress than the creep tests, where deformation is produced mainly by intracrystalline processes. The stress-relaxation curves in Figure 6 show no indication of being concave upward, as would be expected if relaxation occurred at constant structure. Thus, except for the unlikely event that σ_μ is a very small fraction of the applied stress, relaxation involves recovery, and n obtained from the relaxation tests should correspond to that obtained from a series of creep tests at various stress levels. This is true of the data obtained in this study. The results of linear regression analyses on the relaxation data are given in Table 2 for exponential and power law relations between strain rate and stress at constant temperature. Because of the small range of stress, there is no statistical difference between the two descriptions of the data. The mean slope $C/\ln(10)$ using the exponential description, is 3.58 kb^{-1} $\log_{10}$ sec^{-1}.

It has been found from triaxial tests (Rutter, 1974) that a slope, $C/\ln(10)$, in the range of 3 to 4 kb^{-1} $\log_{10}$ sec^{-1} in the exponential description appears to be characteristic for the thermally activated deformation of a range of calcite rocks at 400°C to 500°C at stress

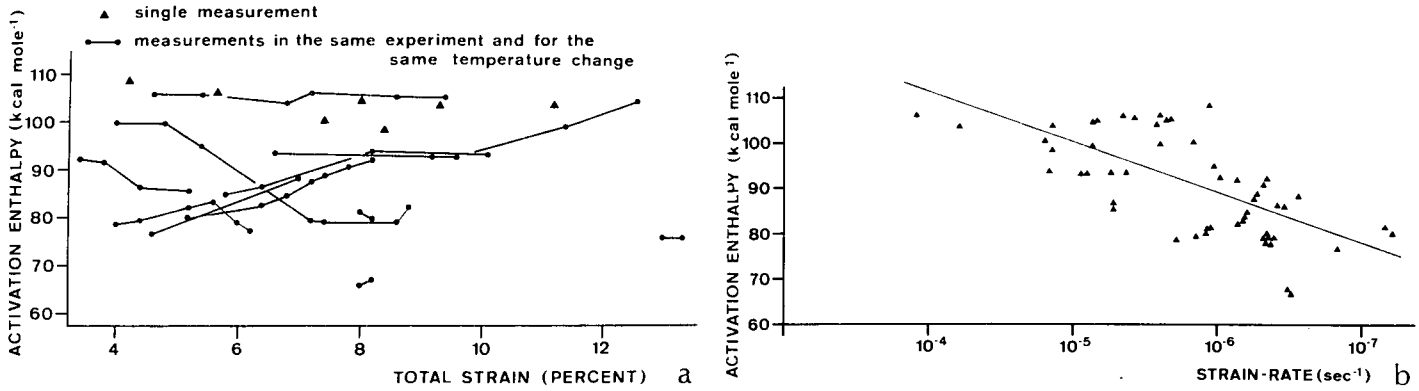

Figure 7. Activation enthalpies for creep determined from differential temperature creep tests (a) as a function of total strain and (b) as a function of strain rate.

levels about 800 bars. In respect to the values of $C/\ln(10)$ and to the stress levels supported at strain rates of $\sim 10^{-8}$ sec^{-1} at 500°C, the uniaxial deformation data are consistent with the results of triaxial tests. Thus, by analogy with data from triaxial tests performed at pressures too high to permit cataclastic flow, it may be inferred that uniaxial deformation of dry Solnhofen limestone at 500°C, at strain rates of the order of 10^{-9}sec^{-1} or less, or at higher strain rates at higher temperatures takes place by purely intracrystalline processes.

It is known that the rate of diffusion-controlled creep is related to hydrostatic pressure through the effect of pressure on diffusivity. This effect, however, is very slight over the range of pressures being considered here (Weertman, 1968) when compared with the potential influence of pressure on microfracturing, which in turn has been argued as unimportant in low strain-rate uniaxial experiments on this rock.

Examination of Deformed Specimens

Figure 9a shows the external appearance of a typical specimen deformed under uniaxial conditions. There is bulging of the sides and a lack of obvious evidence of cataclastic deformation. Samples were also examined by scanning electron microscopy (SEM) (Fig. 9b). The appearance of the specimen is similar to samples of the rock deformed at high temperatures under confining pressure (Fig. 9c). No evidence of recrystallization or grain growth was found, neither was there any evidence of widespread cataclastic deformation that can be recognized with the eye and by SEM in samples deformed at room temperature under moderate confining pressure (Fig. 9d).

Cataclastic flow is usually accompanied by substantial pore-volume increase, whereas intracrystalline flow takes place at constant volume or may even involve syntectonic pore compaction (Edmond and Paterson, 1972). The total porosity of samples deformed to about 12 percent strain — under (1) uniaxial conditions and (2) triaxial conditions at both high and low temperatures — was determined so that comparisons could be made. The initial porosity of the rock was 5.8 percent. Triaxial deformation at 200°C and 500°C at 1.5 kb confining pressure produced final porosities of 8.3 percent and 7.4 percent, respectively. In these instances, the deformation was believed to be mainly intracrystalline. Triaxial deformation at 20°C at 1.5 kb confining pressure produced a final porosity of 12.1 percent. The most strongly deformed central portion of this sample was rendered lighter than normal in color and was more friable than the undeformed rock. Cataclastic flow was clearly important in this sample. Five specimens deformed under high-temperature uniaxial conditions produced final porosities ranging from 6.4 percent to 8.5 percent.

It was recognized that offloading of samples after testing introduces porosity. However, the similarities in rheological behavior, SEM characteristics, and final porosity, between Solnhofen limestone specimens deformed both with and without confining pressure, point to a dominant role of intracrystalline plasticity in both cases.

Little is known about the mechanism of intracrystalline deformation in Solnhofen limestone. Examination by transmission electron microscopy (Barber and Wenk, 1973) of samples deformed under confined conditions (Wenk and others, 1973) has shown that twinning, dislocation multiplication, and glide processes are important during intracrystalline deformation of this material.

GEOLOGICAL IMPLICATIONS

If the experimentally determined slope, $C/\ln(10) = 3.58$ kb^{-1} $\log_{10}$ sec^{-1}, for the exponential stress-strain rate description is used to extrapolate the 500°C strength data to an assumed geological strain rate of 3×10^{-14} sec^{-1}, this limestone would support a differential stress of about 350 bars, provided gross structural changes, such as recrystallization, did not occur and if the possible effects of recovery on the flow law parameters outside experimental conditions are neglected. At lower temperatures the strength would be even higher. It is quite probable, too, that at some stress between 0.5 and 1.5 kb, there is a transition to power law creep. Following Heard and Raleigh (1972), the most likely figure for the stress exponent is about 8. Should such a transition occur, then a still higher stress would be obtained from the extrapolation to geological conditions. Price (1970) has argued that 500 bars would be a relatively high figure for the strength of a rock during orogenesis. Solnhofen limestone, therefore, would appear to be a strong rock over geologic periods of time under low- to medium-grade metamorphic conditions. It is assumed that Nabarro-Herring creep will not be important in limestones deformed at geologic strain rates. Heard

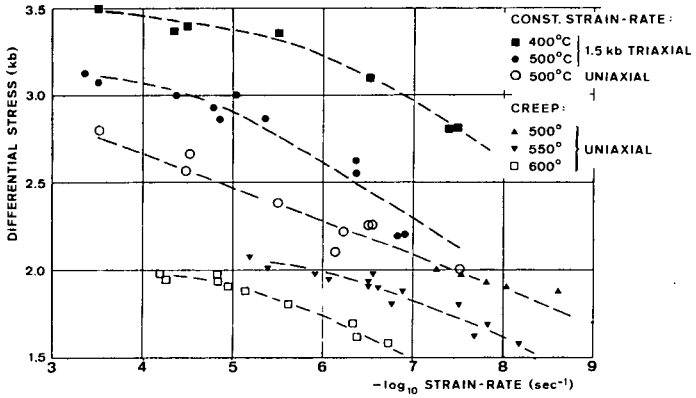

Figure 8. Plot of differential stress at 8 percent total strain against $-\log_{10}$ strain rate, for all creep tests; all uniaxial constant strain-rate tests; and triaxial tests on Solnhofen limestone from the same block, at 1.5 kb confining pressure (previously unpublished results). Dashed lines show trend of each isotherm.

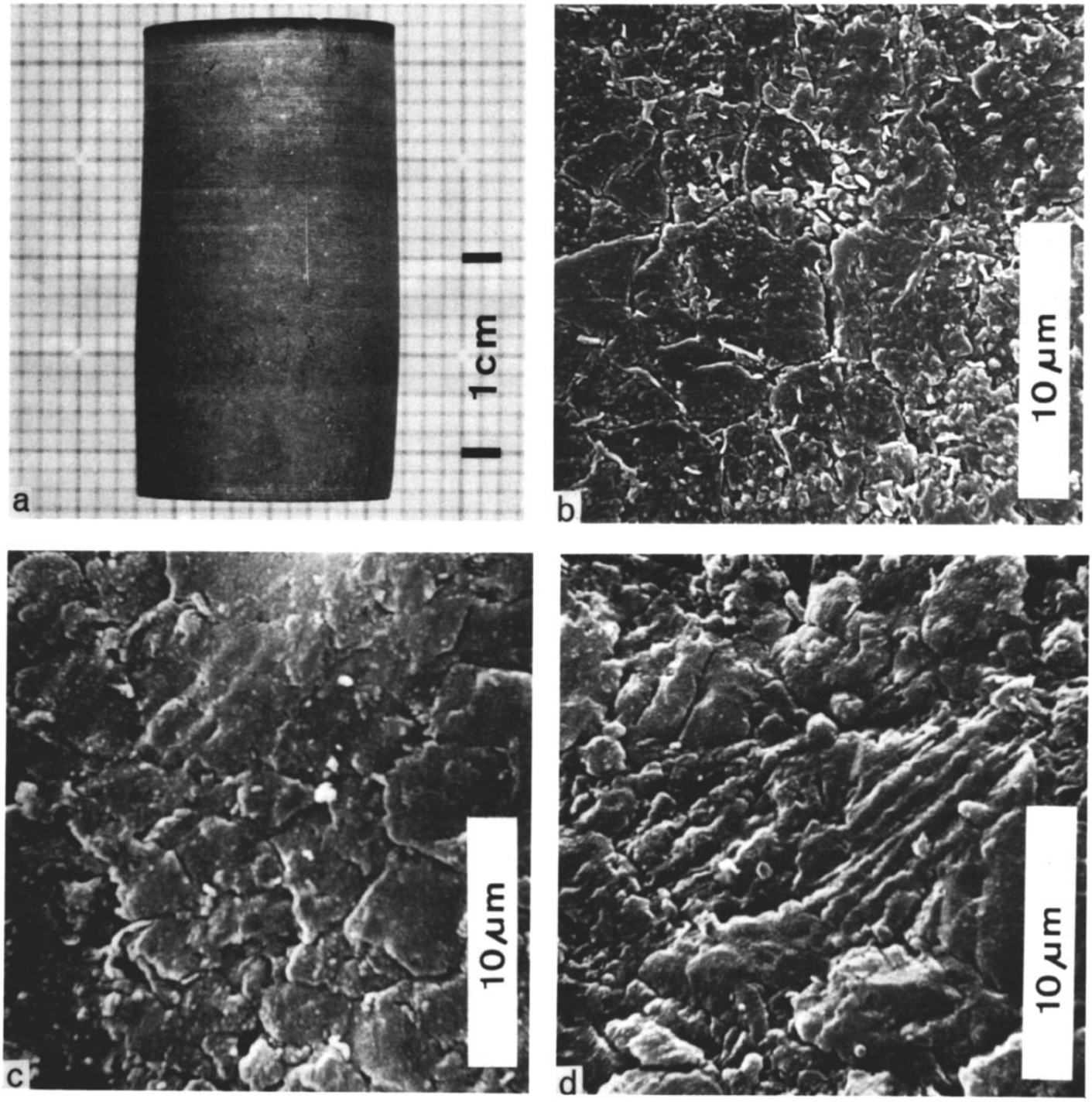

Figure 9. (a) Photograph of deformed sample B.21.C., deformed 6.2 percent referred to the original length. The strain is 12 percent at the maximum width of the specimen. (b) Scanning electron micrograph of Solnhofen limestone deformed under high temperature unconfined conditions, sample B.23.C. (c) Scanning electron micrograph of Solnhofen limestone deformed at 400°C with 1.5 kb confining pressure. (d) Scanning electron micrograph of Solnhofen limestone deformed at 20°C with 600 bars confining pressure.

and Raleigh (1972) argued that a limestone even as fine grained as our sample (20 μm) would not exhibit Nabarro-Herring creep below 650°C at a strain rate of 3×10^{-14} sec^{-1}.

It is probable that under conditions where dislocation motion is the main strain-producing process, coarse-grained marbles tend to be weak, and fine-grained limestones tend to be strong. Thus, flow under small stress differences would be favored by recrystallization and grain growth, the rate of which is accelerated by high temperatures. Wenk and others (1973) observed the onset of syntectonic grain growth in Solnhofen limestone at about 900°C in short-term experiments. The elimination of point defects, which reduce dislocation mobility as a result of recrystallization or grain growth, must be considered as a contributory weakening factor in comparing the behavior of limestones and marbles.

Fine-grained limestones have persisted, however, during orogenic deformations, presumably at temperatures less than 500°C, and have accumulated large strains (though not necessarily at the intracrystalline level), for example, the Lochseiten calc-

mylonite, which lies in the Glarus thrust zone of the Swiss Alps. In the Devonian limestones of southwest England, it can be demonstrated that pressure solution, rather than intracrystalline flow, was responsible for the accumulation of most of the strain (Sorby, 1855, 1879; Ramsay, 1967, p. 196), but it may be noted that the Lochseiten calc-mylonite also contains profusely developed stylolite lamellae similar to those across which shortening has taken place in the Devonian limestones. Both rocks were deformed at temperatures no higher than 400°C; thus, pressure solution in these calcite rocks at a given stress level must be faster than intracrystalline flow at low to intermediate temperatures.

Kehle (1970) argued that some overthrust masses are translated via shear strains in a "viscous" layer in the thrust zone. It is widely believed that a large proportion of the displacement along the Glarus thrust (35 km) has been accommodated by internal deformation of the Lochseiten calc-mylonite (1 to 2 m thick; Hsü, 1969). Bearing in mind that there is a close textural similarity between Solnhofen limestone and Lochseiten calc-mylonite, intracrystalline deformation alone cannot be responsible for the bulk of the strain in the latter rock. It can be argued that the high strength, which may be characteristic of such fine-grained limestones, will not permit shear strains corresponding to the total displacement on the overthrust to accumulate in the time available for the overthrusting to take place (resulting shear strain rate around 10^{-10} sec^{-1}; Schmid, 1974) at differential stress levels below about 1.0 kb. Internal deformation would have to proceed by some faster mechanism, if no frictional sliding occurred.

CONCLUSIONS

1. The high-temperature creep behavior of Solnhofen limestone is similar in many respects to the thermally activated deformation of pure metals, which can be described by a constitutive flow law of the form of equation (1). In particular, the instantaneous creep rate is independent of the previous thermal history, and the activation enthalpy is independent of strain in transient and steady-state creep, at least over limited temperatures and at constant stress.

2. The high strain-rate results appear to have been complicated by fracturing, but the low strain-rate behavior converges toward that typical of deformation by purely intracrystalline processes, which can be studied in high-temperature triaxial experiments.

3. Neglecting the possible effects of recovery on the experimentally determined flow law parameters, extrapolation of the strength data for this rock to geological strain rates yields stress values for intracrystalline flow that are probably high compared with stress values likely to occur in nature. At high temperatures the extrapolation may be invalidated by recrystallization and grain growth, and at lower temperatures there may be a transition to flow by other mechanisms that can operate at differential stresses lower than those required for intracrystalline deformation, for example, pressure solution in a suitable pore-fluid environment.

ACKNOWLEDGMENTS

This work was undertaken during a study visit by Schmid to Imperial College for one year, and financial support from the Zentenarfonds der ETH Zurich is gratefully acknowledged. Equipment used for the experiments was constructed through financial support from the Natural Environment Research Council. J. G. Ramsay, N. J. Price, and A. G. Milnes critically read the manuscript, and R. F. Holloway assisted with the construction of the apparatus.

REFERENCES CITED

Anderson, T. F., 1969, Self diffusion of carbon and oxygen in calcite by isotope exchange with carbon dioxide: Jour. Geophys. Research, v. 74, p. 3918–3931.

——1972, Self diffusion of carbon and oxygen in dolomite: Jour. Geophys. Research, v. 77, p. 857–861.

Barber, D. J., and Wenk, H. R., 1973, The microstructure of experimentally deformed limestones: Jour. Materials Science, v. 8, p. 500–508.

Carter, N. L., and Avé Lallemant, H. G., 1970, High temperature flow of dunite and peridotite: Geol. Soc. America Bull., v. 81, p. 2181–2202.

Dorn, J. E., 1957, The spectrum of activation energies for creep, *in* Creep and recovery: Cleveland, Ohio, Am. Soc. Metals, p. 255–283.

Edmond, J. M., and Paterson, M. S., 1972, Volume changes during the deformation of rocks at high pressures: Internat. Jour. Rock Mech. Min. Sci., v. 9, p. 161–182.

Garofalo, F., 1965, Fundamentals of creep and creep rupture in metals: New York, N.Y., MacMillan Co., 258 p.

Heard, H. C., 1960, Transition from brittle to ductile behavior in Solnhofen limestone as a function of temperature, confining pressure and interstitial fluid pressure: Geol. Soc. America Mem. 79, p. 193–226.

——1963, The effect of large changes in strain rate in the experimental deformation of Yule marble: Jour. Geology, v. 73, p. 162–195.

Heard, H. C., and Raleigh, C. B., 1972, Steady state flow in marble at 500°C to 800°C: Geol. Soc. America Bull., v. 83, p. 935–956.

Heard, H. C., and Rubey, W. W., 1966, The tectonic implications of gypsum dehydration: Geol. Soc. America Bull., v. 80, p. 927–952.

Hsü, K. J., 1969, A preliminary analysis of the statics and kinetics of the Glarus overthrust: Eclogae Geol. Helvetiae, v. 62, p. 143–154.

Hubbert, M. K., and Rubey, W. W., 1959, Role of fluid pressure in the mechanics of overthrust faulting: Geol. Soc. America Bull., v. 70, p. 115–206.

Kehle, R. O., 1970, Analysis of gravity sliding and orogenic translation: Geol. Soc. America Bull., v. 81, p. 1641–1664.

Li, J.M.C., 1967, Dislocation dynamics in deformation and recovery: Canadian Jour. Physics, v. 45, p. 493–509.

McCrum, N. G., and Pearce, D. L., 1973, Determination of activation energy for creep by T-jump in absence of κ-effect: Nature Physical Science, v. 243, p. 52–54.

Price, N. J., 1970, Laws of rock behavior in the earth's crust, *in* Somerton, H., ed., Symposium on rock mechanics, 11th, Berkeley, California: Am. Inst. Mining, Metall., and Petroleum Engineers, p. 3–23.

Price, N. J., and Hancock, P. L., 1972, Development of fracture cleavage and kindred structures: Internat. Geol. Cong., 24th, Montreal 1972, Proc., sec. 3, p. 584–592.

Raleigh, C. H., and Kirby, S. H., 1970, Creep in the upper mantle: Mineral Soc. America Spec. Paper, v. 3, p. 183–190.

Raleigh, C. B., and Paterson, M. S., 1965, Experimental deformation of serpentinite and its tectonic implications: Jour. Geophys. Research, v. 70, p. 3965–3985.

Raleigh, C. B., Kirby, S. H., Carter, N. L., and Avé Lallemant, H. G., 1971, Slip and the clinoenstatite transformation as competing processes in enstatite: Jour. Geophys. Research, v. 76, p. 4011–4022.

Ramsay, J. G., 1967, Folding and fracturing of rocks: New York, McGraw-Hill Book Co., 568 p.

Rutter, E. H., 1972a, The effects of strain rate changes on the strength and ductility of Solnhofen limestone at low temperatures and confining pressures: Internat. Jour. Rock Mech. Min. Sci., v. 9, p. 183–190.

——1972b, On the creep testing of rocks at constant stress and constant force: Internat. Jour. Rock Mech. Min. Sci., v. 9, p. 191–195.

——1972c, The influence of interstitial water on the rheological behaviour of calcite rocks: Tectonophysics, v. 14, p. 13–33.

——1974, The influence of temperature, strain rate and interstitial water in the experimental deformation of calcite rocks: Tectonophysics, v. 22, p. 311–344.

Schmid, S., 1974, The Glarus overthrust: Field data and mechanical model: Eclogae Geol. Helvetiae (in press).

Sorby, H. C., 1855, On slaty cleavage, as exhibited in the Devonian limestones of Devonshire: Philos. Mag., v. 11, p. 20–37.

——1879, Structure and origin of limestones: Geol. Soc. London Proc., v. 35, p. 56–93.

Weertman, J., 1968, Dislocation climb theory of steady state creep: Am. Soc. Metals Trans., v. 61, p. 681–694.

Wenk, H. R., Venkitsubramanyan, C. S., and Baker, D. W., 1973, Preferred orientation in experimentally deformed limestone: Contr. Mineralogy and Petrology, v. 38, p. 81–114.

Manuscript Received by the Society October 1, 1973
Revised Manuscript Received April 25, 1974